Microscale *p*H regulation by splitting water

Li-Jing Cheng[a] and Hsueh-Chia Chang
*Advanced Diagnostics and Therapeutics Initiative, Department of Chemical and
Biomolecular Engineering, University of Notre Dame, Notre Dame, Indiana 46556, USA*

We present a simple, flexible approach for *p*H regulation in micro-chambers by injecting controllable amounts of protons and hydroxide ions via field-enhanced dissociation of water molecules. Under a DC voltage bias, the polymeric bipolar membranes integrated in microfluidics devices generate and separate H^+ and OH^- ions without gas production or contaminant generation resulting from electron-transfer reactions. Robust local on-chip *p*H and *p*H gradients are sustained with no need of additional acidic/basic solutions that dilute analyte concentrations. The method could provide a better strategy for *p*H control in microfluidics. © *2011 American Institute of Physics*. [doi:10.1063/1.3657928]

I. INTRODUCTION

Control of *p*H in microscale environments offers many intriguing possibilities for several biological applications such as on-chip microbioreaction (proteolysis, protein crystallization, etc.,) (Ref. [1]) and cell or biomolecular separation.[2] Several techniques have been developed for *p*H actuation in microfluidic devices including carbon dioxide dissolution,[3] regulation of acid and base solutions,[4] and electrolysis of water by embedded electrodes.[5,6] These methods, however, are either difficult to miniaturize or require microvalves to control the flow of different *p*H solutions.[4,7,8] Electrolysis produces hydrogen and oxygen bubbles that impede microfluidic flow and other reaction products that contaminate the sample. To overcome the aforementioned obstacles, we present an alternative microfluidic *p*H actuator by using field-enhanced water dissociation in microscale bipolar membranes, composed of adjoining cation and anion exchange layers in integrated microfluidic chips. The excess protons and hydroxide ions are generated by directly stripping water molecules apart at the junction of the bipolar membrane, where a high electric field exists due to ion depletion by a reverse voltage-bias.[9] Without any electron-transfer reaction to generate gas, the process produces H^+ and OH^- ions more efficiently than electrolysis. The resulting H^+ and OH^- ions can be separated and injected into nanoliter or smaller volumes of fluid in a microfluidic chip. As the generated ions significantly increase the conductivity of the device, the amount of H^+ or OH^- ions generated can be controlled by monitoring the electric current, thus allowing precise feedback control of the local *p*H and *p*H gradient on the chip. In contrast to the conventional way of changing *p*H by adding acidic or alkaline solutions, the injection of H^+ or OH^- ions does not alter the total solution volume in the microfluidic chip and can hence adjust the *p*H level without diluting the analyte concentration.

Bipolar membranes separating two electrolyte solutions exhibit a rectification property analogous to that observed in a semiconductor p-n diode. While the rectification effect of microfluidic bipolar membranes or nanofluidic devices has been widely studied,[10–14] its water splitting effect has yet to be explored and exploited in microfluidics. The DC current-voltage (I-V) curve exhibits high ionic conductance at forward polarization when the cathode connects to the anion exchange membrane and high resistance at small reverse bias followed by low resistance due to electric field-enhanced water dissociation that generates additional ions at large

---

[a]Author to whom correspondence should be addressed. Electronic mail: lcheng3@nd.edu.

reverse bias.[15–17] Water splitting only commences beyond a threshold reverse bias after the charged mobile species are removed from the junction of the two ion-exchange layers, forming an ion depletion region with a thickness of a few Debye lengths. With almost the entire applied voltage drop occurring across this short distance, the bipolar membrane junction possesses a strong electric field of the order of MV/cm. According to Onsager's theory of the second Wien effect,[18] the water dissociation rate constant is enhanced by a strong electric field while the recombination rate is not. Water molecules, therefore, dissociate into protons and hydroxide ions at the highly reverse-biased bipolar membrane junction only after the ions are depleted there to produce a high field locally.[19,20] Water splitting was also observed in solid oxide nanofluidic devices.[21] In addition to electric fields, it was proposed that water splitting can be elevated by protonation and deprotonation of charged groups in the ion-exchange membranes.[22–25]

II. EXPERIMENT

A. Materials

Sodium silicate, diallyldimethylammonium chloride (DADMAC) (65% w/w in water), 2-acrylamido-2-methyl-1-propanesulfonic acid (AMPS), N,N'-methylenebisacrylamide, 3-trimethoxysilyl propylmethacrylate, 2,2-dimethoxy-2-phenylacetophenone, and [3-(Methacryloylamino)propyl]dimethyl(3-sulfopropyl)ammonium hydroxide inner salt were purchased from Sigma-Aldrich and Hydrion pH indicator solution (UI-100) were from Micro Essential Lab. All the chemicals were used as received.

B. Glass microfluidic chips

Microfluidic channels with the depth of $25\,\mu$m were fabricated on a 1 mm thick glass slide using buffer HF (1:10) etching with the protection of Cr/Au (50 nm/200 nm thick) etching mask. After removing the metal layers and drilling inlet holes, the glass substrate were Piranha cleaned (H_2O_2:$H_2SO_4 = 3$:7) for 10 min and bonded to a bare glass slide which has been Piranha cleaned and spin-coated with sodium-silicate solution (12% v/v) at 2000 rpm. The bonded chips were than clamped and baked at 90 °C in a N_2 oven for at least 5 h.

C. On-chip bipolar membrane

The bonded glass microfluidic channels were flashed with 0.1 M NaOH solution followed by deionized (DI) water rinsing to remove sodium silicate residue on the glass surfaces and surface functionalization with 3-trimethoxysilyl propylmethacrylate (1% in methanol) which allows covalent attachment of acrylated membranes to the glass surfaces. The microscale bipolar membranes were photolithographically defined in the microfluidic channels by exposing aqueous prepolymer mixtures to i-line UV light (365 nm) at 15 mW/cm^2 for 3-6 s through a photomask. The charged monomer in the prepolymer mixture is contributed by either positively charged DADMAC (65% w/w in water), or a negatively charged AMPS (70% in water). Each of the prepolymer solution contains cross-linker, N, N'-methylenebisacrylamide (2% w/w), and photoinitiator, 2,2-dimethoxy-2-phenylacetophenone (1.5% w/w). The weight ratio of the monomer prepared in the mixture provides a final fixed charge density of about 2 M in each ion exchange membrane. After rinsed with DI water to remove the unpolymerized solution from channels, the microfluidic chips were complete with the connection of tubings and reservoirs.

D. Salt bridge electrode

The salt bridge electrode uses an ion permeable membrane to physically isolate a Pt electrode and its surrounding electrolyte from the active sample solution while maintaining their electrical connection. The membrane was fabricated at the end of a pipette tip by photopolymerizing a mixture of $4\,\mu$l prepolymer solution containing zwitterionic monomer [3-(Methacryloylamino)propyl]dimethyl(3-sulfopropyl)ammonium hydroxide inner salt solution (96% w/w in

water), cross-linker N,N'-methylenebisacrylamide (2% w/w), and photoinitiator 2,2-dimethoxy-2-phenylacetophenone (2% w/w). To enlarge the membrane surface area and hence its ion conductance, the pipette tip was trimmed to yield a large orifice. After exposure to 302 nm UV light for 5 min (ca. 1 mW/cm^2), the membrane was completely polymerized forming a well-sealed septum. The salt bridge electrode was complete with a Pt electrode and a filling electrolyte solution.

E. Characterization and Imaging

A *p*H dye mixture consisting of 99% Universal *p*H indicator (Hydrion) and 1% 1 M KCl solution was used to identify the *p*H change in microfluidic devices. The flow rate was controlled by a syringe pump. The current-voltage characteristics were measured through Pt electrodes by HP 4140. The color images were captured using an inverted microscope (IX71, Olympus, Japan) equipped with a color CCD camera (SPOT Insight 2 Megapixel CCD color digital camera) and analyzed by image processing to estimate the corresponding *p*H values. Since a high concentration of *p*H indicator solution was used here, the color response was found to match the indicator color chart for Hydrion *p*H paper strips better than the chart provided for Universal *p*H indicator solutions which is more suitable for aqueous samples with much diluted *p*H indicator.

III. RESULTS AND DISCUSSION

A. On-chip *p*H actuation using bipolar membranes

The UV-polymerized bipolar membrane shown in Fig. 1(a) is composed of a negatively charged poly(2-acrylamido-2-methyl-1-propanesulfonic acid) (pAMPS) layer as a cation exchange membrane on the right side and a positively charged poly(diallyldimethyl-ammonium chloride) (pDADMAC) layer as an anion exchange membrane on the left side, bridging two microfluidic channels. Based on the amount of charged monomer prepared in the prepolymer mixtures, both membranes were synthesized to contain about 2 M concentration of fixed charge. When incubated in a *p*H indicator solution, a mixture of bromothymol blue, methyl red, and thymol blue, the anion exchange membrane is stained dark blue due to the trapping of negatively charged bromothymol blue in a strong alkaline environment. However, little *p*H dye was found in the cation exchange membrane. Under a bias of Vm = −30 V, *p*H fronts can be observed in the microfluidic channel due to the generation of excess protons and hydroxide ions at the membrane junction with the high electric field. The bipolar membrane exhibits unique electrical features in reverse bias, as shown in the cyclic I-V curve (Fig. 1(b)) measured in a 10 mM KCl solution with the cyclic voltage swept at a rate of 0.5 V/s. Its I-V characteristic at reverse bias can be divided into three regimes as indicated in Fig. 1(b): a hysteresis regime (regime 1) at low reverse bias, in which the current amplitude increases linearly and then drops precipitously when the voltage is swept from zero to negative values but decreases monotonically at a lower conductance for a voltage sweep from negative to zero; a low conductance regime (regime 2); and at high voltage, a water splitting regime (regime 3) in which the excess protons and hydroxide ions contribute to the elevated ion current. The hysteresis effect at low reverse bias is most likely due to ion migration transients within the cation and anion exchange membranes. When the voltage is swept from zero to negative, the counter ions are depleted from the membrane junction and migrate out of the membrane. This ion migration can take time. Without much change in the counter ion concentration during the initial interval, the conductance remains constant resulting in an ohmic behavior. When the ions at the membrane junction are completely depleted at a more negative voltage bias, the bipolar membrane becomes very resistive and the current amplitude returns to a lower level. This low-level current is carried mostly by the minority co-ions in each membrane. As illustrated in Fig. 1(c), the bipolar membrane preserves the low ionic conductance until the electric field at the depletion region is large enough to generate additional charge carriers by enhancing the dissociation of water molecules into H$^+$ and OH$^-$ ions. Greater current amplitude is obtained with the increase
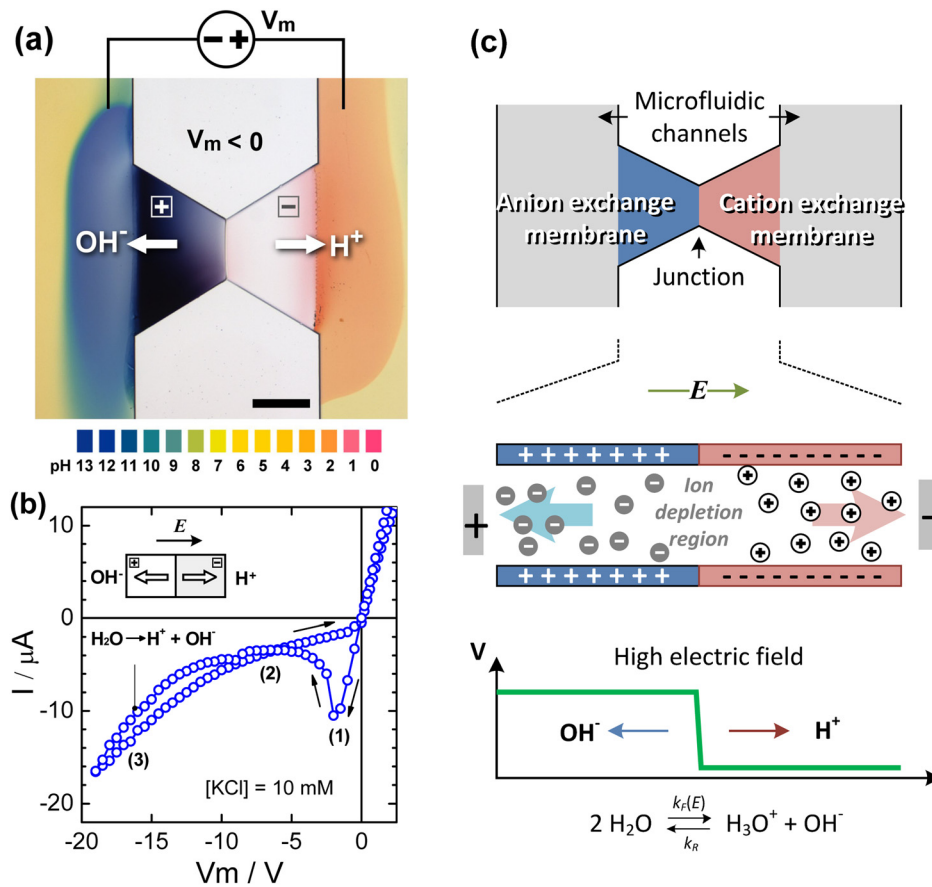
FIG. 1. (a) pH actuation in microfluidic channels was achieved by splitting water into protons and hydroxide ions from a reverse-biased (Vm = −50 V) microscale polymeric bipolar membrane. Positive and negative symbols indicate the fixed charges in pDADMAC and pAMPS membranes, respectively. The scale bar is 300 μm. (The video of Figure 1(a) can be found in the supplementary material.) The pH values were estimated by Universal pH indicator. (b) I-V characteristics at re-vere bias Field-enhanced water dissociation was observed in the increase of current at the reverse-bias region (Vm < −10 V) in the I-V curve. The numbers (1), (2), and (3) indicate the three distinct regimes in the I-V curve—hysteresis regime, saturation regime and water splitting regime, respectively. (c) When the anode connects to the anion exchange membrane, the voltage bias depletes the ions from the bipolar membrane junction creating a local electric field as high as several MV/cm theoretically. Under such a large field, the dissociation rate $k_F(E)$ of water molecules increases significantly; as a result, they tend to split into protons and hydroxide ions.

of reverse voltage bias, implying more dissociation of water molecules. With a reverse voltage scan from negative to zero, the water splitting effect is alleviated and counter ions constantly refill the membranes, shrinking the depletion region at the membrane junction. However, since the depletion region exists for any reverse bias, the bipolar membrane retains a low ionic conductance. As a result, the I-V curve does not follow the forward path in the backward voltage sweep, forming a hysteresis loop at low reverse bias. The size of the hysteresis loop depends on the scanning rate as well as the geometry of the membrane. The data are not presented here. Depending on the quality of polymerization, in general, the on-chip bipolar membranes were found to exhibit stable condition for water breaking in hydrated state for more than a month. The devices lasting for more than 5 weeks after fabrication were not tested. The bipolar membrane works properly in a wide range of ionic strength between two extreme conditions: DI water and an ionic strength close to 2 M. When the ion concentration is less than μM (10^{-6} M) i.e., close to deionized condition, the microfluidic channel becomes resistive and can hardly couple enough voltage across the bipolar membrane. On the other hand, with the ionic strength close to the concentration of the fixed charge in the membrane, i.e., 2 M in this device, the membrane becomes less permselective and therefore cannot split water efficiently.

To gain more insight into how the H^+ and OH^- ions are generated, the dynamics of field-enhanced water dissociation at high reverse bias was visualized in a *p*H dye-stained bipolar membrane. By taking advantage of the dye's affinity for the anion exchange membrane and its low mobility there, we monitored the generation and propagation of OH^- ion flux in the membrane. As mentioned, the bromothymol blue from the *p*H indicator stains the anion exchange membrane blue due to its high *p*H condition. To improve the color contrast of the newly generated OH^- ions, we converted the membrane's background color from blue to green by incubating the device with 1 mM HCl solution before test for 3 min to lower its *p*H level. Proton fluxes were not observable in cation exchange membranes because of the insufficient *p*H dye in this membrane. Fig. 2 shows the sequential images captured at 10-s intervals right after a 30 V reverse bias was applied. It can be seen that under the reverse bias (Vm = −30 V, measured current ∼36 μA), a blue band with elevated OH^- ion concentration emerges at the membrane junction and propagates across the 500 μm long anion exchange membrane. At the reverse bias of 30 V, it takes about 40 s for the device to generate and pump OH^- and H^+ ions into microfluidic channels with a velocity of about 13 μm/s. The propagation time reduces to less than 10 s when a reverse bias of 65 V is applied.

The video in the supplementary material[26] shows the electrokinetic dynamics of a voltage-biased bipolar membrane composed of adjoining anion exchange membrane on top (containing positively charged ammonium groups) and cation exchange membrane on bottom (containing negatively charged sulfonic groups). Each membrane is 500 μm long. To observe *p*H change, the microchannels are filled with *p*H indicator solution which shows yellow in color. Because of the charge of the *p*H dye molecules, the anion exchange membrane is stained blue. Depending on the polarity of voltage bias applied across the bipolar membrane, the ion can get depleted or enriched inside/outside the membrane due to membrane polarization. When applied a 5 V forward bias with anode connecting to the cation exchange membrane, large ion current passes through the bipolar membrane (refer to the I-V curve in Fig. 1(b)) due to the enrichment of ion in the membrane junction. The enrichment of ions also induces slight swelling of the membrane because of the increase of osmotic pressure. Meanwhile, ion depletion occurs outside the membranes leading to the removal of the yellowish *p*H dye molecules, which are also charged, and formation of vortices. When applied a −15V reverse-bias with anode connected to the anion exchange membrane, ion depletion happens at the membrane junction, lowering the osmotic pressure. In consequence, the membrane slightly shrinks and starts to perform water splitting at its junction where a large electric field locates. Little amount of alkaline solution is produced and injected in the top microchannel, whereas the acidic solution is too diluted to observe. When a large 50 V reverse voltage bias is applied, a greater electric filed drops across the membrane junction and hence splits more water molecules into H^+ and OH^-, resulting in the increase of ion current (refer to the I-V curve in Fig. 1(b)). It is worthwhile to note that, the membrane junction flaps at the onset of the voltage bias due to the triggering of the osmotic pressure inside the membrane. Following the actuation, a purple colored OH^- flood emerges from the junction and propagates across the anion exchange membrane. The H^+ flood is not observable until it flows out into the bottom microchannel which contains *p*H dyes. H^+ ions are released earlier than OH^- ions because of its higher electrophoretic mobility.
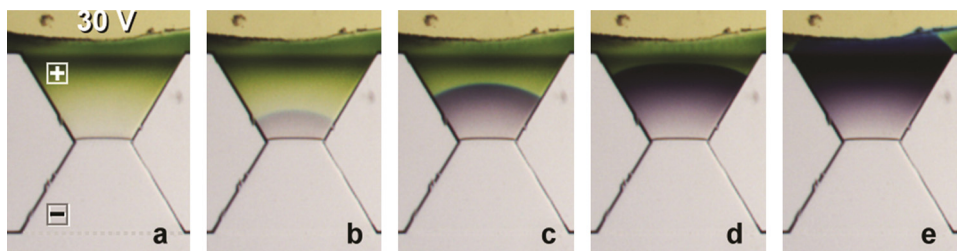

FIG. 2. Dynamics of hydroxide ion generation from field-enhanced water dissociation at bipolar membrane junction under a reverse bias of 30 V. The images were captured with time interval of 10 s. Scale bar indicates 300 μm.

The speed of the H^+/OH^- generation and injection is primarily determined by the time required to drug the counter ions out of the bipolar membrane, which is equivalently to the discharge of a capacitor. To speed up the process, one could reduce the bipolar membrane capacitor by shrinking its length and cross section area.

B. Regulation of constant *p*H conditions in microfluidics

Generation and separation of H^+/OH^- ions by bipolar membranes and their distinct electrical signatures suggest a new microfluidic *p*H regulation strategy. As shown in Fig. 3(a), a microfluidic device uses separate voltage control of two bipolar membranes placed beside the upstream microchannel and a downstream microfluidic mixer as shown in the microscopic image in Fig. 3(b). The two sets of bipolar membrane were arranged in such a way that H^+ or OH^- ions can be injected independently from one of the two bipolar membranes to the fluid delivered from the left side. The amount of each ion pumped into the microchannel is tunable by controlling the voltage biases, V_H and V_{OH}. Note that the voltage sources V_H and V_{OH} were connected in a way that positive voltages refer to reverse biases which are opposite to the polarity of Vm in Fig. 1(a). The corrugated pattern fabricated by wet etching was designed to create chaotic mixing of solutions in microchannels. With different combination of V_H and V_{OH}, the device produces various ratios of H^+ and OH^- ions upstream and well mixes them up through the mixer to achieve divergent *p*H conditions uniformly distributed in the downstream. Under a flow rate of 2 μl/min, five particular *p*H conditions, approximately *p*H 3,5,7,9, and 11, were successfully demonstrated in Fig. 3(c) by applying corresponding V_H and V_{OH} listed in the figure to electrically adjusting the H^+/OH^- ion currents. The variation of fluid *p*H level can be observed by the color of *p*H indicator as H^+ or OH^- ions are added and mixed in the microchannel. Although the controllable *p*H variation demonstrated here is quite large, it is possible to achieve finer *p*H control based on the adjustment of electrical currents. So far the *p*H measurement in the microfluidic devices is based on the color of the *p*H indicator which itself has
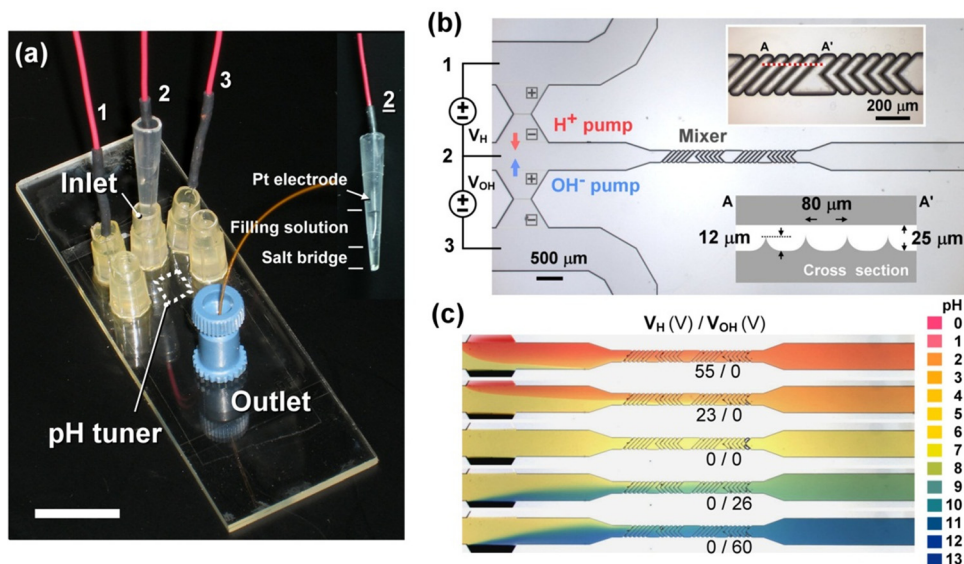

FIG. 3. (a) Bipolar membrane-based microfluidic *p*H tuner enables *p*H adjustment by separately controlling the voltage biases across two upstream bipolar membranes via three Pt electrodes in the reservoirs. In electrode 2, a salt-bridge is used to prevent direct contact with the sample solution. The inset shows the configuration of the salt-bridge electrode 2. Scale bar is 1 cm. (b) *p*H actuation in microfluidics with two sets of upstream bipolar membrane serving as proton and hydroxide ion pumps. The numbers in the circuit indicate the corresponding electrodes in (a). The insets show the zoom-in image and the illustrated cross-section (not in scale) of the mixer channel. (c) By adjusting the voltages V_H and V_{OH}, various *p*H conditions can be generated in microfluidic channels by mixing different fractions of protons or hydroxide ions under a flow rate of 2 μl/min. The resulting *p*H values are estimated to be 3, 5, 7, 9 and 11 from top to bottom, according to the *p*H chart.
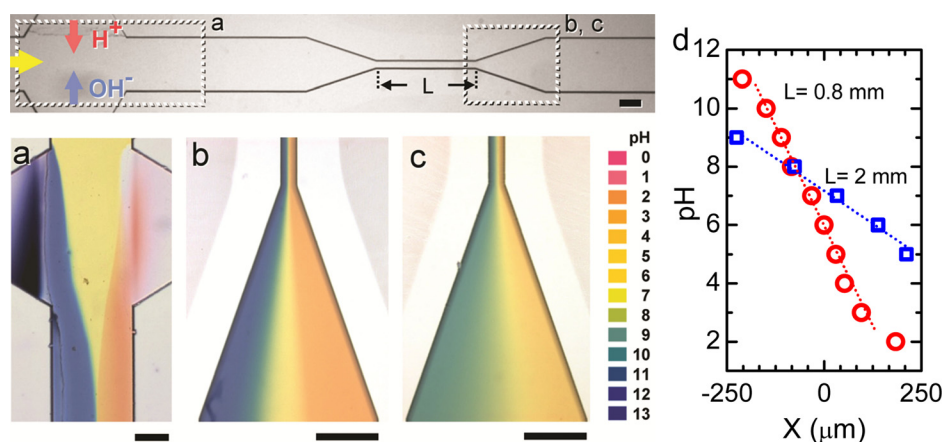
FIG. 4. (a) Abrupt *p*H profile builds up near the *p*H actuators upstream. Different *p*H gradients were generated across a 500 μm wide channel downstream after passing through a 0.8 mm long (b) or a 2 mm long (c), 50 μm wide narrowed channel. The scale bars in images indicate 200 μm. (d) *p*H profiles across the downstream of channel in (b) and (c).

limited *p*H resolution. Once we can integrate a micro-*p*H sensor in the device, we shall be able to determine the limitation of *p*H variation we can adjust.

C. Generation of stable *p*H gradients across flow chambers

Apart from constant *p*H control, the development of stable *p*H gradients under flow conditions in microfluidic devices is important for several applications such as isoelectric focusing for molecular separation. We demonstrated in Fig. 4 a robust variable-range, linear *p*H gradient across a 500 μm wide microchannel. With simultaneous injection of both H$^+$ and OH$^-$ ions ($V_H = 32$ V, $V_{OH} = 35$ V), two extreme *p*H conditions separated by an abrupt boundary were formed in the upstream microchannel (Fig. 4(a)). When the liquid passed through a 50 μm wide necked microchannel, its *p*H profile redistributed to form a linear gradient due to dispersion. The narrowed microchannel was designed to reduce the lateral diffusion length. Depending on the flow rate and the length of the narrowed channel, the lateral diffusion time can be adjusted to create *p*H gradients over different ranges. Figures 4(b) and 4(c) show two *p*H profiles produced after passing a neutral *p*H solution through a 0.8 mm and a 2 mm long narrowed channel, respectively, under the same flow rate of 2 μl/min. With a shorter diffusion time in the 0.8 mm long channel, the acidic and alkaline solutions were less mixed, yielding a wide-range *p*H gradient covering approximately from *p*H 2 to 11. The 2 mm long narrow channel provided longer diffusion time and hence created smoother *p*H gradient (about *p*H 5-9). The *p*H values across the microchannel are summarized in Fig. 4(d). The *p*H gradient can be scaled up to centimeter-scale which is not shown here. The resultant *p*H gradient is found to be mainly contributed by the lateral diffusion in the narrowed microchannel rather than in the downstream fan-structured microchannel which can only slightly improves the gradient profile by further dispersion.

IV. CONCLUSION

We demonstrated electrokinetic control of fluid *p*H and generation of stable *p*H gradients by using field-enhanced water dissociation in microfluidics. Split directly from water molecules at a reverse-biased bipolar membrane junction, H$^+$ and OH$^-$ ions are produced without suffering from gas and contaminant generation during water electrolysis. By electrically controlling two independent H$^+$ and OH$^-$ ions injection rates into a single stream, various *p*H conditions can be created without the addition of acidic or basic solutions, which requires sophisticated flow control and dilutes the sample solution. Offering several advantages over conventional methods, the novel strategy of *p*H regulation outlined in this work should enable better control

of chemical reactions in microreactors and the robust pH gradient generation should improve the performance of molecular separation in microfluidic isoelectric focusing devices.

ACKNOWLEDGMENTS

[1] M. Samorski, G. Muller-Newen, and J. Buchs, Biotechnol. Bioeng. **92**, 161 (2005).
[2] D. Kohlheyer, J. C. D. Eijkel, S. Schlautmann, A. van den Berg, and R. B. M. Schasfoort, Anal. Chem. **79**, 8190 (2007).
[3] C. Christian Läritz and L. Page, Sens. Actuators, A **84**, 230 (2000).
[4] H. L. T. Lee, P. Boccazzi, R. J. Ram, and A. J. Sinskey, Lab Chip **6**, 1229 (2006).
[5] H. Corstjens, H. A. H. Billiet, J. Frank, and K. C. A. M. Luyben, Electrophoresis **17**, 137 (1996).
[6] K. Macounova, C. R. Cabrera, M. R. Holl, and P. Yager, Anal. Chem. **72**, 3745 (2000).
[7] H. Suzuki and R. Yoneyama, Sens. Actuators B **96**, 38 (2003).
[8] H. Hosono, W. Satoh, M. Toya, K. Morimoto, J. Fukuda, and H. Suzuki, Sens. Actuators B **132**, 614 (2008).
[9] K. N. Mani, J. Membrane Sci. **58**, 117 (1991).
[10] O. J. Cayre, S. T. Chang, and O. D. Velev, J. Am. Chem. Soc. **129**, 10801 (2007).
[11] J.-H. Han, K. B. Kim, H. C. Kim, and T. D. Chung, Angew. Chem. **48**, 3830 (2009).
[12] L.-J. Cheng and L. J. Guo, Chem. Rev. Soc. **39**, 923 (2010).
[13] H.-C. Chang, and G. Yossifon, Biomicrofluidics **3**, 012001 (2009).
[14] Z. Slouka, M. Přibyl, D. Šnita, and T. Postler, Phys. Chem. Chem. Phys. **9**, 5374 (2007).
[15] I. C. Bassignana and H. Reiss, J. Membrane Sci. **15**, 27 (1983).
[16] G. Grossman, J. Phys. Chem. **80**, 1616 (1976).
[17] R. Simons and G. Khanarian, J. Membrane Biol. **38**, 11 (1978).
[18] L. Onsager, J. Chem. Phys. **2**, 599 (1934).
[19] H. Strathmann, J. J. Krol, H.-J. Rapp, and G. Eigenberger, J. Membrane Sci. **125**, 123 (1997).
[20] S. Mafe and P. Ramfrez, Acta Polym. **48**, 234 (1997).
[21] L.-J. Cheng and L. J. Guo, ACS Nano **3**, 575 (2009).
[22] I. Rubinstein, A. Wrshawsky, L. Schechtman, and O. Kedem, Desalination **51**, 55 (1984).
[23] R. Simons, Desalination **28**, 41 (1979).
[24] R. Simons, Electrochim Acta **29**, 151 (1984).
[25] R. Simons, Electrochim Acta **30**, 275 (1985).
[26] See supplementary material at http://dx.doi.org/10.1063/1.3657928 for electrokinetic dynamics of field-enhanced water dissociation in a bipolar membrane.